

Modeling the magnetospheres of luminous stars: Interactions between supersonic radiation-driven winds and stellar magnetic fields^{a)}

Stan Owocki,^{b)} Rich Townsend, and Asif ud-Doula^{c)}

Bartol Research Institute, University of Delaware, Newark, Delaware 19716

(Received 2 November 2006; accepted 4 January 2007; published online 22 March 2007)

Hot, luminous stars (spectral types O and B) lack the hydrogen recombination convection zones that drive magnetic dynamo generation in the sun and other cool stars. Nonetheless, observed rotational modulation of spectral lines formed in the strong, radiatively driven winds of hot stars suggests magnetic perturbations analogous to those that induce “co-rotating interaction regions” in the solar wind. Indeed, recent advances in spectropolarimetric techniques have now led to direct detection of moderate to strong (100–10 000 G), tilted dipole magnetic fields in several hot stars. Using a combination of analytic and numerical magnetohydrodynamic models, this paper focuses on the role of such magnetic fields in channeling, and sometimes confining, the radiatively driven mass outflows from such stars. The results show how “magnetically confined wind shocks” can explain the moderately hard x-ray emission seen from the O7V star Theta-1 Ori C, and how the trapping of material in a “rigidly rotating magnetosphere” can explain the periodically modulated Balmer line emission seen from the magnetic B2pV star Sigma Ori E. In addition, magnetic reconnection heating from episodic centrifugal breakout events might explain the occasional very hard x-ray flares seen from the latter star. The paper concludes with a brief discussion on the generation of hot-star fields and the broader relationship to other types of magnetospheres. © 2007 American Institute of Physics. [DOI: 10.1063/1.2472340]

I. INTRODUCTION

Massive, luminous, hot stars have strong, radiatively driven stellar winds (see Refs. 1 and 2), with flow speeds ranging up to 1% of the speed of light, and mass loss rates ranging up to 10^9 times that of the solar wind. Their high surface temperatures mean that such stars lack the hydrogen recombination convection zone that induces the magnetic dynamo cycle of cooler, solar-type stars (e.g., Ref. 3). Hot stars have thus been classically treated as having a hydrostatic radiative envelope that is nonmagnetic and spherically symmetric, suggesting that their dynamical, radiatively driven stellar wind should likewise be nonmagnetic, spherically symmetric, and steady state.

In fact, however, spectroscopic monitoring of lines formed in such hot-star winds show them to be generally quite variable, commonly exhibiting discrete absorption components that typically recur on timescales comparable to the stellar rotation period (see, e.g., Refs. 4 and 5). Such wind modulation could well be the result of a weak to moderate magnetic field at the stellar surface, which induces faster and slower wind streams that the stellar rotation causes to collide in spiral co-rotating interaction regions (see Refs. 6–8), much as is observed *in situ* for the solar wind (see Ref. 9).

Indeed, over the years spectropolarimetric measurements have led to direct detection of quite strong fields in some hot stars. A first example was the detection (see Ref. 10) of a strong (~ 10 kG), oblique-dipole magnetic field in the

helium-strong B2p star σ Ori E. Subsequent observations of other members of this helium-strong class (so named on account of their elevated photospheric He abundances) revealed similar-strength fields in several additional objects (see Ref. 11). In recent years, advances in spectropolarimetric techniques have led to the discovery of weaker fields in other early-type systems, including Be emission-line stars (e.g., ω Ori; Ref. 12), slowly pulsating B stars (e.g., ζ Cas; Ref. 13), and the more massive O-type stars (e.g., θ^1 Ori C; Ref. 14). In conjunction with the indirect evidence from wind-line variability, it now seems plausible that most or even *all* hot stars might harbor magnetic fields, albeit at levels that fall below historical and present-day detection thresholds.

In most cases these polarimetry observations are well fit by a simple dipole surface field with an axis that is tilted by some fixed angle β relative to the stellar rotation axis. The dipole nature and relative constancy of the inferred field amplitude and orientation—in some cases extending now over three decades—seems clearly to preclude the kind of active convective dynamo that gives rise the magnetic activity cycles in solar-type stars. As such, the source of hot-star fields remains uncertain, with suggested possibilities ranging from a fossil origin (as in Ref. 15), to slow buoyant diffusion to the surface of fields generated in the star’s convective core (as in Refs. 16 and 17).

We review here our recent efforts to develop dynamical models for the effects of such a surface dipole field on the radiatively driven mass outflow. The next section applies magnetohydrodynamic simulations of a *magnetically confined wind shock* (MCWS) first model developed by Babel and Montmerle (Refs. 18 and 19) to explain x-ray emission observed by *Rosat* (see Ref. 20) from the magnetic O7V star

^{a)}Paper N12 5, Bull. Am. Phys. Soc. 51, 180 (2006).

^{b)}Invited speaker. Electronic address: owocki@bartol.udel.edu

^{c)}Also at Department of Physics and Astronomy, Swarthmore College, Swarthmore, PA 19801.

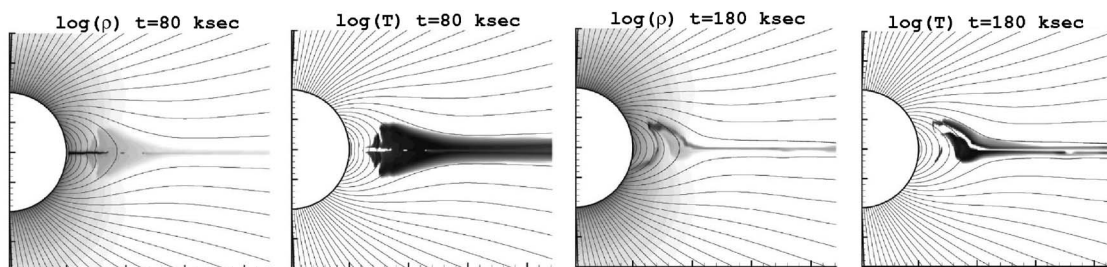


FIG. 1. MHD simulations of the MCWS model for θ^1 Ori C, showing the logarithmic density ρ and temperature T in a meridional plane. Left: at a time 80 ks after the initial condition, the magnetic field has channeled wind material into a compressed, hot disk at the magnetic equator. Right: at a time 180 ks, the cooled equatorial material is falling back toward the star along field lines, in a complex “snake” pattern. The darkest areas of the temperature plots represent gas at $T \sim 10^7$ K, hot enough to produce relatively hard x-ray emission of a few keV. Animations of these simulations are available for download from Ref. 36.

θ^1 Ori C. We then discuss the role of magnetic fields in spinning up the wind outflow from a rotating star, emphasizing that this does *not* produce the *magnetically torqued disk* (MTD) proposed by Cassinelli *et al.* (Ref. 21) as a mechanism for producing the orbiting, Keplerian disks inferred from the characteristic Balmer line emission in Be stars. We next show, however, that the very strong magnetic fields of Bp stars can lead to a *rigidly rotating magnetosphere* (RRM) (as discussed in Ref. 22), with rigid-body disks or clouds that can explain quite well the observed Balmer emission in Bp stars such as σ Ori E. We further show that the eventual centrifugal breakout of such material can lead to strong heating from magnetic reconnection, which thus could explain the very hard x-ray flares seen from this star (see Ref. 23). Finally, we conclude with a summary and future outlook, including a brief discussion of how the relatively modest perturbation of a weaker magnetic field might explain the rotational modulation observed in the wind lines of most hot stars.

II. MHD SIMULATIONS OF WIND OUTFLOWS FROM MAGNETIC HOT STARS

We have applied the ZEUS-3D MHD code (for details of the code, see Ref. 24) to two-dimensional (2-D), nonrotating, axisymmetric simulations of the dynamical interplay between a dipole stellar magnetic field and a line-driven, hot-star wind (discussed in Refs. 8, 25, and 26). A key result is

that the overall effectiveness of magnetic fields in channeling the stellar wind outflow can be characterized by the ratio of the magnetic to wind energy densities,

$$\eta(r) \equiv \frac{B^2/8\pi}{\rho v^2/2} = \eta_* \frac{(r/R_*)^{2-2q}}{(1 - R_*/r)^\beta}. \quad (1)$$

Here, $\eta_* \equiv B_*^2 R_*^2 / (\dot{M} v_\infty)$ defines an overall “magnetic confinement parameter” in terms of the strength of the equatorial field B_* at the stellar surface radius R_* , and the wind terminal momentum $\dot{M} v_\infty$. The latter equality in Eq. (1) isolates the radial variation in terms of a magnetic power-law index q ($=3$ for a dipole) and a velocity index β (≈ 1 for a standard line-driven wind model developed in Ref. 2).

A general point here is that, because the energy density of the dipole field declines much more steeply with radius ($\sim 1/r^6$) than does the wind density ($\sim 1/r^2$), the wind always dominates the outer regions, forcing open the fields into a nearly radial configuration. However, for large confinement parameter $\eta_* \gg 1$, the magnetic field can still dominate in the inner wind, channeling the flow along closed loop lines toward the magnetic equator, where the collision between material from opposite hemispheres can form strong, x-ray emitting shocks. As shown by simulation results in Figs. 1 and 2, the transition between the radial outflow of the outer wind from the closed-loop confinement of the inner wind occurs roughly at the *Alfvén radius* R_A , where the mag-

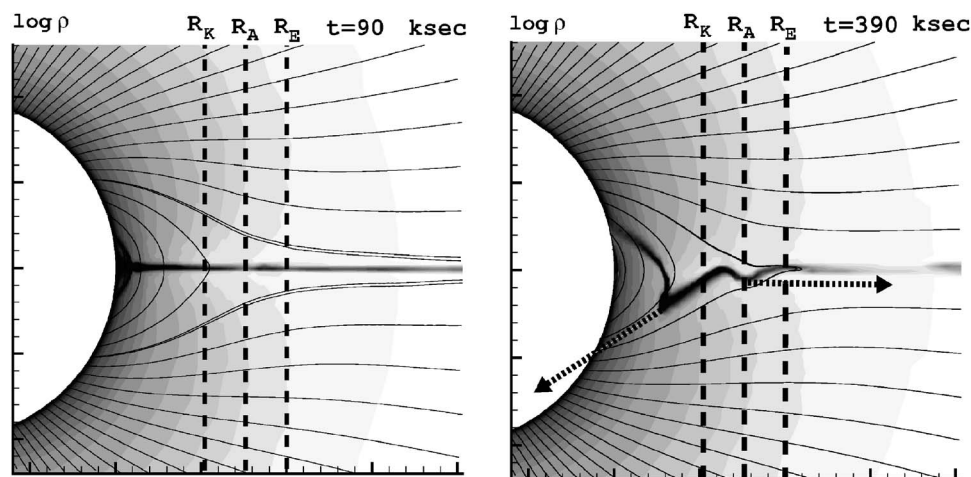


FIG. 2. Density of a 2-D MHD simulation for a model with $\eta_* = 10$ and $W = 1/2$, shown at time snapshots of 90 ks (left) and 390 ks (right) after a dipole field is introduced into an initially steady-state, unmagnetized, line-driven stellar wind. The curves denote magnetic field lines, and the vertical dashed lines indicate the equatorial location of the Keplerian, Alfvén, and escape radii defined in Eqs. (2), (4), and (5) of the text. The arrows denote the upward and downward flow above and below the Keplerian radius, emphasizing that the material never forms a stable, orbiting disk.

netic and wind energy densities are equal [$\eta(R_A) \equiv 1$]. Neglecting the wind velocity variation, the case of a dipole field gives the explicit estimate

$$R_A \approx \eta_*^{1/4} R_* \quad (2)$$

The initial MHD simulations by ud-Doula and Owocki (see Ref. 25) assumed, for simplicity, that radiative heating and cooling would keep the wind outflow nearly isothermal at roughly the stellar effective temperature. However, to model the x-ray emission from shocks that form from the magnetic channeling and confinement, subsequent efforts (see Refs. 26 and 27) have relaxed this simplification to include a detailed energy equation that follows the radiative cooling of shock-heated material. In particular, building upon the initial suggestion by Babel and Montmerle (see Ref. 19) that such *magnetically confined wind shocks* (MCWS) might explain the relatively hard x-ray spectrum observed by *Rosat* for the O7V star θ^1 Ori C, Gagné *et al.* (see Ref. 27) have recently applied such energy-equation, MHD simulations toward a detailed, dynamical model of the more extensive *Chandra* x-ray observations of this star. Based on the recent spectropolarimetric measurement (see Ref. 14) of about a 1100 G dipole field for θ^1 Ori C, combined with empirical and theoretical estimates of the wind momentum and stellar radius, the simulations assume a moderately large magnetic confinement parameter; i.e., $\eta_* \approx 10$.

Figure 1 illustrates results at two time snapshots, representing, respectively, a relatively early, simple phase ($t = 80$ ks; left two panels), and a typical later, more complex phase ($t = 180$ ks; right two panels). In each figure, the gray-scales represent the spatial distribution of logarithmic density (first and third panels) and logarithmic temperature (second and fourth panels), with superposed lines representing the magnetic field. After introduction of the field, the left panels show the initial wind response is to stretch open the field lines in the outer region, but to be channeled toward the magnetic equator by the closed loops in the inner region. Within these closed loops, the flow from opposite hemispheres collides to make strong, x-ray emitting shocks, yielding a nearly symmetric structure that, at this time snapshot, is quite similar to what was predicted in the semi-analytic, fixed-field models of Babel and Montmerle (Ref. 19). However, such a simple, symmetric compression is only transient, lasting only a few 10 ks, after which it evolves to the much more complex structure shown in the right panels of Fig. 1. This is because once shocked material at the tops of loops cools, its support against gravity by the magnetic tension along the convex field lines is inherently unstable, leading to a complex pattern of fall back along the loop lines down to the star. However, when averaged over time [which here might roughly substitute for averaging over azimuth in a more realistic three-dimensional (3-D) simulation], the overall level of x-ray emission turns out to be quite similar to what is obtained from the simple, symmetric state represented by the left panels of Fig. 1.

Overall, the associated x-ray emission of this MHD model matches quite well the key properties of the *Chandra* observations for θ^1 Ori C (see Ref. 27), including: the relatively hard x-ray spectrum that arises from the high post-

shock temperatures $T \sim 20\text{--}30$ MK; the relative lack of broadening or blueshift from x-ray lines emitted from the nearly static, shock-heated material; and the x-ray light curve eclipse that stems from the moderate source radius $r \approx 1.5R_*$ for the bulk of the x-ray emission.

III. WIND SPIN-UP FROM DIPOLE ALIGNED WITH STELLAR ROTATION AXIS

Let us next examine the nature of magnetic channeling for the winds from rotating hot stars, with particular emphasis on whether a large-scale magnetic field could spin-up the stellar wind outflow into a “magnetically torqued disk” (MTD), as advocated by Cassinelli *et al.* (Ref. 21). As noted above, MHD simulations (see Refs. 25 and 26) indicate that a dipole magnetic field can confine the flow within closed loops that extend out to about the Alfvén radius; i.e., $R_A \approx \eta_*^{1/4} R_*$. In rotating models, such closed loops tend also to keep the outflow in rigid-body rotation with the underlying star, so that R_A also roughly represents the radius of maximum rotational spin-up of the wind azimuthal speed.

To further characterize such rotational effects, let us thus now define a *Keplerian co-rotation radius* R_K at which rigid-body rotation would yield an equatorial centrifugal acceleration that just balances the local gravitational acceleration from the underlying star,

$$\frac{GM}{R_K^2} = \frac{v_\phi^2}{R_K} = \frac{V_{\text{rot}}^2 R_K}{R_*^2}, \quad (3)$$

where V_{rot} is the stellar surface rotation speed at the equator. This can be solved to yield

$$R_K = W^{-2/3} R_*, \quad (4)$$

where $W \equiv V_{\text{rot}}/V_{\text{crit}}$, with $V_{\text{crit}} \equiv \sqrt{GM/R_*}$ the critical rotation speed. Note, moreover, that co-rotation out to an only slightly higher *escape radius*,

$$R_E = 2^{1/3} R_K = 2^{1/3} W^{-2/3} R_*, \quad (5)$$

would imply an azimuthal speed that equals the local escape speed from the star’s gravitational field.

The above scalings suggest that a likely necessary condition for propelling outflowing material into a Keplerian disk is to choose a combination of parameters for magnetic confinement versus stellar rotation such that $R_K < R_A < R_E$. As a sample test case, we focus here on the specific combination $\eta_* = 10$ and $W = 1/2$, which gives the sequence $\{R_K, R_A, R_E\} = \{1.59, 1.78, 2\} R_*$, and which thus should represent an optimal case for any possible magnetic spin-up into Keplerian orbit.

Figure 2 illustrates results of 2-D MHD simulations for this case, using the approach and general model assumptions described in ud-Doula and Owocki (Ref. 25), but now extended to include field-aligned rotation. The left panel shows that conditions at a time 90 ks after introduction of the field do superficially resemble a magnetically torqued disk. Closer examination shows, however, that most of this equatorial compression does not have the appropriate velocity for a stable, stationary, Keplerian orbit. Thus, in just a few kiloseconds of subsequent evolution, this putative “disk” be-

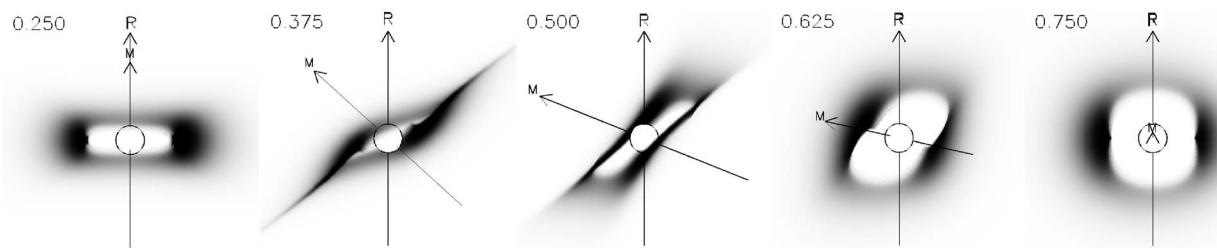


FIG. 3. Maps of the optically thick $H\alpha$ emission from circumstellar plasma in an RRM model for σ Ori E, plotted at five consecutive phases of the stellar rotation cycle (indicated at the top left of each panel). The field confining the plasma is a rigid dipole tilted by an angle $\beta=67^\circ$ to the rotation axis, and then decentered by $0.3R_*$ in a direction perpendicular to both magnetic and rotation axes, the latter being shown by arrows labeled “M” and “R,” respectively. The observer is situated at an inclination $i=70^\circ$ to the rotation axis, and the disk of the star (whose emission is neglected in the plots) is shown by a circle. Note that the circumstellar emission is dominated by two clouds, edge-on at phase 0.25 and face-on at phase 0.75. Color animations complementary to these maps are available for download from Ref. 36.

comes completely disrupted, characterized generally by infall of the material in the inner region, i.e., below the Keplerian radius R_K , and by outflow in the outer region above this Keplerian radius. The right panel illustrates the irregular form of the dense compression at an arbitrarily chosen later time (390 ks from the initial start). The arrows emphasize the flow divergence of the dense material both downward and upward from the Keplerian radius. This evolution is most vividly illustrated through animations, which are available from Ref. 36.

We have carried out similar MHD simulations for a moderately extensive set of combinations for the rotation and magnetic confinement parameters. In all cases we find that any equatorial compressions are dominated by radial inflows and/or outflows, with no apparent tendency to form a steady, Keplerian disk.

IV. THE RIGIDLY ROTATING MAGNETOSPHERE MODEL FOR STRONGLY MAGNETIC HOT STARS

The above MTD scenario was proposed to explain to the Keplerian disks inferred from the characteristic Balmer line emission of Be stars. The general lack of rotational modulation in such Be-star line emission implies a overall axisymmetry that requires any magnetic field (which are not generally detected) producing a putative MTD would have to have a dipole axis closely aligned with the stellar rotation axis, as indeed was assumed in the above MHD simulations. By contrast, the so-called Bp stars do often exhibit clear rotational modulation in circumstellar emission lines, along with very strong magnetic fields (several kG) that are inferred to have a dipole axis that is tilted by some angle β relative to the rotation axis.

For example, in the prototypical Bp star σ Ori E, the magnetic field is estimated to have a dipole surface strength $B \sim 10^4$ G and tilt angle $\beta \approx 45^\circ - 70^\circ$, with a comparable observer’s inclination $i=45^\circ$, leading to modulation of Zeeman polarization on a rotation period of 1.19 day (see Ref. 28). Coupled with a relatively low mass-loss rate ($\dot{M} \sim 10^{-10} M_\odot \text{ yr}^{-1}$), this implies an extremely strong magnetic confinement for the wind ($\eta_* \sim 10^7$). Unfortunately, direct MHD simulation of this case is severely complicated by the inherently 3-D nature associated with the nonzero tilt angle β , and by the extreme stiffness of the magnetic field. The

latter implies a very high Alfvén speed, and thus very short Courant timestep, needed to preserve numerical stability within the explicit timestepping of the ZEUS code. Together these considerations make direct MHD simulations of winds from Bp stars such as σ Ori E impractical.

However, by considering the idealized limit of arbitrarily strong confinement ($\eta \rightarrow \infty$), we have recently developed a quite intricate description of the *rigidly rotating magnetosphere* (RRM) that is likely to form in such strongly magnetic, rotating Bp stars. In this limit, the field lines behave like rigid tubes, constraining the outflowing wind plasma along trajectories that are fixed by the *a priori* field geometry. With sufficiently rapid rotation, the outward centrifugal force, arising from the enforced co-rotation of the plasma, can support post-MCWS plasma at the tops of closed magnetic loops, in *magnetohydrostatic* configurations centered on the minima of the effective (centrifugal plus gravitational) potential along each field line. With the steady feeding of wind material from the star, these potential wells should gradually fill with cool plasma, forming a quasi-steady magnetosphere that co-rotates with the star. A strength of this RRM approach is its suitability to *arbitrary* field configurations, not just to the simple axisymmetric case of a rotation-axis-aligned dipole, to which MHD simulations have so far been restricted on the grounds of computational tractability.

Application of the RRM formalism to an oblique-dipole model star, with parameters appropriate to σ Ori E, leads to a specific prediction of the accumulation of wind material in two co-rotating circumstellar clouds, situated at the intersection between magnetic and rotational equators (Ref. 22; see also Fig. 3). This prediction matches quite well the observationally inferred distribution of plasma proposed by Groote and Hunger (Ref. 28) and others. Using techniques we originally developed for spectral synthesis from pulsating hot stars (e.g., Refs. 29 and 30), we have calculated time-resolved $H\alpha$ profiles for the RRM σ Ori E model (see Ref. 31); as we show in Fig. 4, these synthetic profiles exhibit a remarkable degree of agreement with the corresponding observations. A similar level of agreement is found between the predicted optical and IR photometric behavior, and that observed by Hesser *et al.* (Ref. 32).

Recently, we have improved this semi-analytic RRM model by computing hydrodynamic quantities of the wind

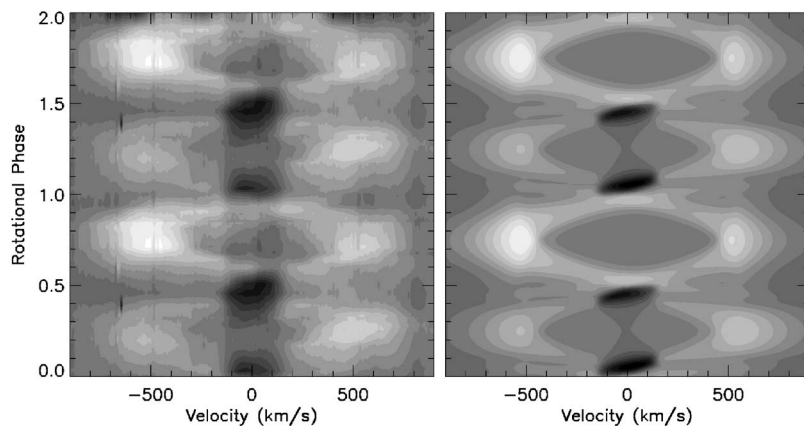


FIG. 4. Time-series spectra of the varying circumstellar H α emission observed from σ Ori E (left; Groote, private communication), phased on the 1.19-day rotation period of the star, compared against the corresponding synthetic data predicted by the RRM model (right; see Fig. 3); white indicates emission relative to the background photospheric H α profile, and black indicates absorption. Note in particular the model's reproduction of the observed double S-wave variability, including the blue/red and temporal asymmetries, and the correct positioning of the eclipse-like absorptions at phases 0.05 and 0.45.

along each rigid-field line fully self-consistently. This allows the wind to evolve in time dynamically. In our preliminary calculations, we find very strong shocks develop around the accumulations surfaces, just as predicted by the semi-analytic RRM model. As the magnetosphere gets filled in, the wind material below Kepler radius collected at the accumulation surfaces, falls back on to the stellar surface, something that the RRM model failed to account for. Such a dynamic behavior of the wind in a strong magnetic field environment is difficult to model by full MHD, as argued earlier. A paper on this hybrid *rigid-field hydrodynamic* (RF-HD) model of the magnetosphere is in preparation.

V. A CENTRIFUGAL BREAKOUT MECHANISM FOR X-RAY FLARING

In routine x-ray observations of σ Ori E by the *Rosat*, *XMM*, and *Chandra* satellites, two of the three approximately day-long exposures showed clear evidence for a quite strong, hard, x-ray flare (see Ref. 33). Such x-ray flaring from an early-type star is unusual and unexpected, and thus was initially attributed instead to an unseen cool companion star (Ref. 34), for which flaring is commonly associated with magnetic reconnection heating arising from the activity of a convective magnetic dynamo. However, the strength and hardness of these flares make it unlikely that they could be produced within the inherent length constraints for magnetic loops from such a cool star (D. Mullan, p.c.), which then suggests that they might in fact be associated with either the Bp star or its immediate circumstellar environment. Similar conclusions can be reached regarding a flare detected in *Chandra* ACIS-I observations of the young O9.5Vpe star θ^2 Ori A (see, for example, Ref. 35). We are therefore confronted with an entirely new instance of x-ray flare production, which—with the absence of deep subphotospheric convection zones in hot stars—appears challenging to explain purely in terms of the traditional mechanisms operative in cooler stars.

Fortunately, the above RRM model can provide a quite natural alternative explanation for the flaring seen in these magnetic hot stars. The steady accumulation of plasma in a RRM cannot continue indefinitely; eventually, circumstellar densities reach levels where the outward centrifugal force must overwhelm the inward magnetic tension forces, leading

to the breakout of plasma from the magnetosphere in a direction perpendicular to the rotation axis. Townsend and Owocki (Ref. 22, see Appendices) present a simple analysis of this breakout for the case of σ Ori E; they find that the largest-scale evacuations can be expected every ~ 100 y, but they also anticipate a whole hierarchy of breakout events extending down to much shorter timescales. During a breakout, the magnetic field lines become so drawn out by the ejected plasma that they snap and then reconnect closer to the star. The energy release associated with this reconnection, and its subsequent dissipation via radiative cooling, represents a strong candidate for the generation of the x-ray flares.

Preliminary tests of this new *centrifugal breakout* mechanism for x-ray production appear quite encouraging. Although it is not yet feasible to conduct MHD simulations at a confinement parameter $\eta_* \sim 10^7$ appropriate to σ Ori E (for the reasons noted earlier, relating to the Courant condition), we have constructed models for a moderately confined ($\eta_* \sim 600$) case, rotating at half the critical rate ($W=1/2$) at which the surface gravitational and centrifugal forces would balance along the equator. As illustrated in Fig. 5, the simulations reveal that, after the initial formation of a small rigidly rotating magnetosphere close to the star (as predicted by the RRM model), a semi-regular sequence of breakout events occurs, whereby field lines are pulled out into long, narrow loops, before snapping back toward the star (cf. middle and right panels of Fig. 5). The energy released by the reconnection is sufficient to heat nearby material to temperatures $T \sim 10^8$ K, high enough to produce the hard (≥ 2 keV) components of the flares observed in σ Ori E and θ^2 Ori A.

VI. SUMMARY, CONCLUSIONS, AND FUTURE OUTLOOK

The results here demonstrate that magnetic fields in hot stars with moderate to large confinement parameters ($\eta_* > 1$) can have a substantial effect in channeling their radiatively driven stellar winds. In the example of the recently detected, moderate-strength magnetic field from the slowly rotating O7V star θ^1 Ori C, the MHD simulations of magnetically confined wind shocks provide a quite good match to the observed x-ray properties. The addition of rotation can spin up the wind, but does *not* lead to magnetically torqued

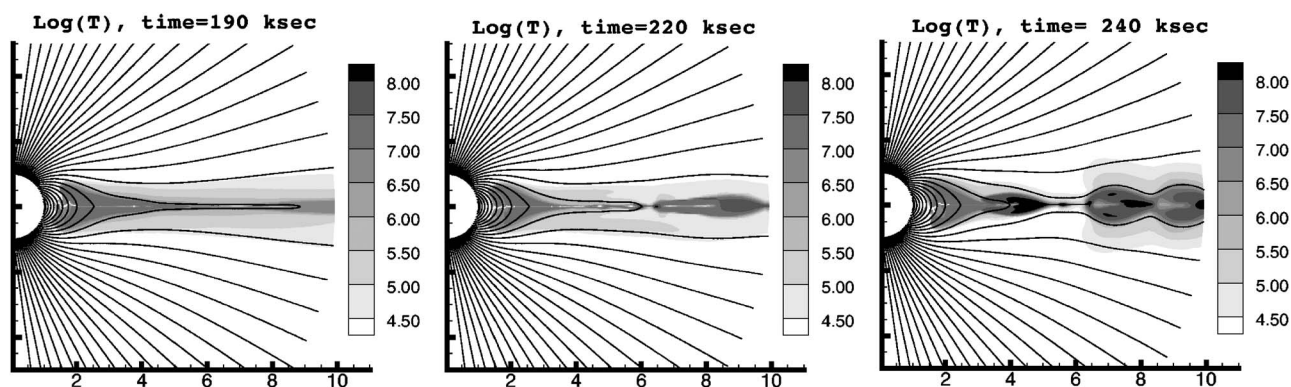


FIG. 5. MHD simulations of a centrifugal breakout model for x-ray flaring, showing the logarithmic temperature T in a meridional plane. Left: at a time 190 ks, the centrifugal force acting on dense material in the equatorial plane has drawn the magnetic field out into a long, narrow neck. Middle: at a time 220 ks, the stressed magnetic field has reconnected, heating material in the outer regions of the equatorial plane to $T \sim 10^8$ K. Right: at a time 240 ks, the reconnected field has snapped back toward the star, producing further heating. Animations of these simulations are available for download from Ref. 36.

disk that could explain the orbiting circumstellar material inferred from the characteristic Balmer emission of Be stars. However, in rotating Bp stars with very strong fields, the channeling of the wind can feed a *rigid-body* disk or clouds, which can be well modeled within a semi-analytic RRM formalism that provides a quite good match to the rotational modulations in line and continuum observations. Moreover, the eventual centrifugal breakout of such material suggests a new mechanism for magnetic reconnection heating to explain observed hard x-ray flares in several such Bp stars.

While the present discussion has focussed mostly on model development for cases with relatively large, detectable fields ($B > 100$ G), it also seems likely that the base perturbations associated with more moderate, still undetected fields could also play a role in the semi-regular variability commonly detected in the UV wind lines of hot stars. To model such modulations from fields that are not symmetric about the stellar rotation axis, future simulations will need to be extended to 3-D. If such MHD models can provide a good match to the observed variability, it would support the notion that, contrary to the classical picture, hot-star magnetic fields are not limited to a few cases or peculiar classes, but are a common, perhaps even ubiquitous, feature. This has potentially quite broad implications, requiring for example that there must be a mechanism for stellar field generation that is quite distinct from the usual convective dynamo operating in the Sun and other cool stars. It might even require reappraisal of our basic assumptions regarding the envelope and interior of early-type stars. The study here of magnetic channeling of hot-star winds represents another illustration of the complex but broad significance of magnetic fields for astrophysical plasmas.

ACKNOWLEDGMENT

This work has been partially supported by NASA grants LTSA-NNG05GC36G and Chandra/TM7-8002X.

¹L. B. Lucy and P. M. Solomon, *Astrophys. J.* **159**, 879 (1970).

²J. I. Castor, D. C. Abbott, and R. I. Klein, *Astrophys. J.* **195**, 157 (1975).

³E. N. Parker, *Astrophys. J.* **122**, 293 (1955).

⁴D. Massa, A. W. Fullerton, J. S. Nichols *et al.*, *Astrophys. J. Lett.* **452**, 53

(1995).

⁵A. W. Fullerton, D. L. Massa, R. K. Prinja, S. P. Owocki, and S. R. Cranmer, *Astron. Astrophys.* **327**, 699 (1997).

⁶D. J. Mullan, *Astrophys. J.* **283**, 303 (1984).

⁷S. R. Cranmer and S. P. Owocki, *Astrophys. J.* **462**, 469 (1996).

⁸S. P. Owocki and A. ud-Doula, *Astrophys. J.* **600**, 1004 (2004).

⁹A. J. Hundhausen, *J. Geophys. Res.* **78**, 1528 (1973).

¹⁰J. D. Landstreet and E. F. Borra, *Astrophys. J.* **224**, L5 (1978).

¹¹E. F. Borra and J. D. Landstreet, *Astrophys. J.* **228**, 809 (1979).

¹²C. Neiner, A.-M. Hubert, Y. Frémat, M. Floquet, S. Jankov, O. Preuss, H. F. Henrichs, and J. Zorec, *Astron. Astrophys.* **409**, 275 (2003).

¹³C. Neiner, V. C. Geers, H. F. Henrichs, M. Floquet, Y. Frémat, A.-M. Hubert, O. Preuss, and K. Wiersema, *Astron. Astrophys.* **406**, 1019 (2003).

¹⁴J.-F. Donati, J. Babel, T. J. Harries, I. D. Howarth, P. Petit, and M. Semel, *Mon. Not. R. Astron. Soc.* **333**, 55 (2002).

¹⁵L. Mestel, *Astron. Soc. Pac. Conf. Ser.* **305**, 3 (2003).

¹⁶P. Charbonneau and K. B. MacGregor, *Astrophys. J.* **559**, 1094 (2001).

¹⁷K. B. MacGregor and J. P. Cassinelli, *Astrophys. J.* **586**, 480 (2003).

¹⁸J. Babel and T. Montmerle, *Astrophys. J. Lett.* **485**, 29 (1997).

¹⁹J. Babel and T. Montmerle, *Astron. Astrophys.* **323**, 121 (1997).

²⁰M. Gagné, J. Caillault, J. R. Stauffer, and J. L. Linsky, *Astrophys. J. Lett.* **478**, 87 (1997).

²¹J. P. Cassinelli, J. C. Brown, M. Maheswaran, N. A. Miller, and D. C. Telfer, *Astrophys. J.* **578**, 951 (2002).

²²R. H. D. Townsend and S. P. Owocki, *Mon. Not. R. Astron. Soc.* **357**, 251 (2005).

²³A. ud-Doula, R. H. D. Townsend, and S. P. Owocki, *Astrophys. J. Lett.* **640**, L191 (2006).

²⁴J. M. Stone and M. L. Norman, *Astrophys. J., Suppl. Ser.* **80**, 791 (1992).

²⁵A. ud-Doula and S. P. Owocki, *Astrophys. J.* **576**, 413 (2002).

²⁶A. ud-Doula, Ph.D. thesis, University of Delaware, 2003.

²⁷M. Gagné, M. Oksala, D. H. Cohen, S. K. Tonnesen, A. ud-Doula, R. H. D. Townsend, S. P. Owocki, and J. J. MacFarlane, *Astrophys. J.* **628**, 986 (2004).

²⁸D. Groote and K. Hunger, *Astron. Astrophys.* **116**, 64 (1982).

²⁹R. H. D. Townsend, *Mon. Not. R. Astron. Soc.* **284**, 839 (1997).

³⁰R. H. D. Townsend, S. P. Owocki, and I. D. Howarth, *Mon. Not. R. Astron. Soc.* **350**, 189 (2004).

³¹R. H. D. Townsend, S. P. Owocki and D. Groote, *Astrophys. J. Lett.* **630**, L81 (2005).

³²J. E. Hesser, P. P. Ugarte, and H. Moreno, *Astrophys. J.* **216**, 31 (1977).

³³D. Groote and J. H. M. M. Schmitt, *Astron. Astrophys.* **418**, 235 (2004).

³⁴J. Sanz-Forcada, E. Franciosini, and R. Pallavicini, *Astron. Astrophys.* **421**, 715 (2004).

³⁵E. D. Feigelson, P. Broos, J. A. Gaffney, G. Garmire, L. A. Hillenbrand, S. H. Pravdo, L. Townsley, and Y. Tsuboi, *Astrophys. J.* **574**, 258 (2002).

³⁶See EPAPS Document No. E-PHPAEN-14-020791 for animations. This document can be reached via a direct link in the online article's HTML reference section or via the EPAPS homepage (<http://www.aip.org/pubservs/epaps.html>).